

# Lawrence Berkeley National Laboratory

## Recent Work

### Title

SELF-TRIGGERED WIRE CHAMBERS FOR RADIATION IMAGING PURPOSES

### Permalink

<https://escholarship.org/uc/item/13d8k5t3>

### Authors

Kaufman, Leon  
Perez-Mendez, Victor  
Sperinde, Johnie M.

### Publication Date

1970-09-01

CD 3

**RECEIVED**  
LAWRENCE  
RADIATION LABORATORY

NOV 10 1970

**LIBRARY AND  
DOCUMENTS SECTION**

SELF-TRIGGERED WIRE CHAMBERS FOR  
RADIATION IMAGING PURPOSES

Leon Kaufman, Victor Perez-Mendez and  
Johnie M. Sperinde

September 1970

AEC Contract No. W-7405-eng-48

**TWO-WEEK LOAN COPY**

*This is a Library Circulating Copy  
which may be borrowed for two weeks.  
For a personal retention copy, call  
Tech. Info. Division, Ext. 5545*

**LAWRENCE RADIATION LABORATORY**  
**UNIVERSITY of CALIFORNIA BERKELEY**

## DISCLAIMER

This document was prepared as an account of work sponsored by the United States Government. While this document is believed to contain correct information, neither the United States Government nor any agency thereof, nor the Regents of the University of California, nor any of their employees, makes any warranty, express or implied, or assumes any legal responsibility for the accuracy, completeness, or usefulness of any information, apparatus, product, or process disclosed, or represents that its use would not infringe privately owned rights. Reference herein to any specific commercial product, process, or service by its trade name, trademark, manufacturer, or otherwise, does not necessarily constitute or imply its endorsement, recommendation, or favoring by the United States Government or any agency thereof, or the Regents of the University of California. The views and opinions of authors expressed herein do not necessarily state or reflect those of the United States Government or any agency thereof or the Regents of the University of California.

SELF-TRIGGERED WIRE CHAMBERS FOR  
RADIATION IMAGING PURPOSES

Leon Kaufman  
University of California  
San Francisco, California 94122

Victor Perez-Mendez  
University of California  
San Francisco, California 94122  
and Lawrence Radiation Laboratory  
Berkeley, California 94720

and

Johnie M. Sperinde  
Lawrence Radiation Laboratory  
Berkeley, California 94720

Summary

Spark chambers with digitized readouts offer distinct advantages in spatial resolution and coverage over other gamma-ray imaging devices. While these chambers usually require external logic signals for triggering, in this paper we describe a method that provides self-triggering spark chambers. We also describe initial tests of a 45 X 45 cm spark chamber with  $^{60}\text{Co}$  and  $^{198}\text{Au}$  samples.

Introduction

The widespread use of gamma-ray-emitting radioisotopes has become a powerful tool in human and animal physiology studies. While present devices for the spatial imaging of isotope distributions tend to be limited both in resolution and area coverage, wire spark chambers with electronic readout afford compact instruments that are able to cover large areas with high resolution and supply quantitative information at low cost.

In our spark chambers the wires in one plane run at 90 deg to the wires in the other so that X and Y coordinates can be obtained (fig. 1), and Mylar windows are used to seal the chamber.

The sampling system consists of a magnetostrictive<sup>1</sup> wire (typically a ferromagnetic alloy) placed close to, but not in contact with, the chamber wires. The particular wire (or wires) carrying current to the spark are surrounded by a rapidly changing magnetic field. The properties of magnetostrictive materials are such that their length varies with magnetic field. The fast increase and decrease of field around the sensor wire produces a rapid contraction and relaxation in that wire. This disturbance travels down the line with acoustic speeds (about 5000 m/sec). A detector consisting of a pickup coil and amplifier produces a signal that is processed by the technique of differentiation and zero crossing so that the center of gravity of the spark current can be determined. The signal is timed by 20 MHz scalers; the number of sparks that can be detected depends on the number of scalers used. To make the system independent of the positioning of the magnetostrictive line and of conditions that affect the speed of sound in that line, we connect the first and last wires in each plane through a resistor-capacitor chain. In this way, a current flows through these wires each time the chamber is pulsed, and two marker or "fiducial" pulses are obtained on the line. The first fiducial turns the timing clocks on, the spark turns one clock off and a second spark or fiducial turns the

other clock off. In the latter case we obtain an absolute normalization of distances along the line.

For a wire-to-wire separation of 1 mm, we obtain location accuracies of  $\pm 0.33$  mm, this being due to the fact that the current splits proportionately to the distances from the track to the two wires that straddle it.

In many experimental situations the range and energy of the detected particles is sufficiently large so that the events are selected by a triggering signal derived from scintillation counters placed strategically around the spark chambers to form an appropriate coincidence for the event. Such a triggering system is less effective in dealing with  $\gamma$  rays or other neutral particles whose presence is detected by secondary charged particles produced in converters in or around the wire planes, and becomes especially inefficient when dealing with low-energy  $\gamma$  rays from radioactive sources, or X-rays, where the range of the secondary electrons is small enough so that they often do not emerge from a single gap.

Since our interest is in using wire chambers for medical diagnostic purposes--the localization of  $\gamma$ -emitting radioactive isotopes with energies ranging from tens of kev to a few Mev--we have investigated the characteristics of the signals produced by low-energy charged particles in the pre-avalanche region in the wire chamber and the sparking characteristics of the chamber itself when triggered by these signals.<sup>2</sup>

Experimental

The spark chamber used to test the properties of gas-multiplication triggering has an active area of 20 cm X 20 cm and a capacity of 140 pF<sup>3</sup>. It consists of three planes, the central one made up by stringing 0.08 mm steel wires 1.5 mm apart over a lucite frame. The outside planes are of copper-etched Mylar, 1 mm apart. The distance between the planes is 1 cm in each case, and magnetostrictive readout is possible from the two outside planes. For operation, the chamber is filled to atmospheric pressure with a 90% Ne - 10% He gas mixture saturated at room temperature with ethyl alcohol (~ 50 mm Hg).

Figure 2 shows the circuit used for particle detection and spark triggering. The outer electrodes are grounded and a positive high voltage was applied to the central one. A 22 M $\Omega$  resistor is used to limit the current available to the chamber and prevent a continuous discharge. The resistor also determines the

recovery time of the chamber for detection of particles after sparking, since it limits the recharging rate of the chamber.

The proportional pulses are collected from the high-voltage electrode through a 100 pF capacitor into a voltage-sensitive preamplifier with an input impedance of 10 k $\Omega$ . The preamplifier has a gain of  $\sim 20$  and its pulses are fed into a variable-gain linear amplifier. The preamplifier is protected during sparking by a simple back-to-back diode system with a 1 k $\Omega$  resistor to limit the current through the diodes. The spark chamber is decoupled by a series gap from the capacitor in the high-voltage pulsing system.

When the chamber is operated with the gas mixture previously described  $\sim 0.25$  mV pulses are obtained for an applied voltage of 3900 V; this corresponds to a gas amplification of approximately 6000. The detection efficiency of the chamber was tested by placing it between two scintillation detectors and counting simultaneously double (between the scintillators only) and triple coincidences. Full efficiency was reached at 3750 V.

Using a variable threshold discriminator set to trigger at 10% of the height of the average pulses, we find that it fires about 0.4  $\mu$ sec after passage of the particle through the chamber. Since no appreciable losses in sparking efficiency are seen for times up to 0.5  $\mu$ sec after passage of the particle (see fig. 3), the delay can be tolerated. The triggering jitter time is less than 0.3  $\mu$ sec. We observed also that the operation of the chamber is moderately insensitive to the rise time of the high-voltage pulse and that rise times of  $\sim 50$  nsec do not cause any loss in efficiency.

We have also measured the rekindling time of this chamber (time during which a spark will be formed along the path of a previous spark, i.e., the number of double sparks on the same track as a function of the delay time between the sparks). This is shown in fig. 4 for a particular set of parameters.

#### A Gamma-Ray Scanner for Clinical Uses

Magnetostrictive readout spark chambers coupled to converters, i.e., lead plates, offer distinct advantages over present systems for the imaging of  $\gamma$ -ray emitting radionuclides: 1 mm or better accuracy of location, large area for whole body scanning, and low cost. Such a system with an active area of 45 X 45 cm is presently being used by us<sup>4</sup>, and the schematics are shown in fig. 5.

When imaging single  $\gamma$ -ray-emitting nuclei, a collimator placed between the source and detector is commonly used. For all practical applications, the resolution of the system is given by the hole size and configuration of the collimator. In our work the chamber is triggered on all counts in the scintillator except the ones blocked by the cosmic-ray anti-coincidence counter. Not all triggers correspond to real events since an appreciable number of  $\gamma$  rays will convert in the scintillator itself, giving rise to false triggers, and conversely, not all electrons reaching the chamber give rise to a trigger signal.

It is in this type of application that full advantages of gas-multiplication-triggered spark chambers are realized, since they allow for detection of particles that would not register otherwise, and an increase in detection efficiency produces a directly proportional increase in sensitivity.

We have performed computer simulations of collimators, and found that for constant resolution, the acceptance (fraction of  $\gamma$  rays being collimated) increases with increasing thickness, since the density of holes can be increased. We have built and tested with <sup>60</sup>Co sources, two 15 cm thick lead collimators with 5 mm diameter holes. The first, which has 5 mm septa, was found to give a granular image, the resolution of the detector making it easy to see each individual hole. The second collimator has 3 mm septa, and individual holes are still discernible, although to a lesser extent than in the previous case. We feel then that 1-2 mm septa will be adequate for 5 mm holes. From these preliminary results, we conclude that for applications where high resolution is desired, collimators with holes as small as 1 mm could be used.

Full advantage of the high resolution and large scanned areas that spark chambers make available can only be realized through the use of computers. Pictures can be obtained on-line by the use of an ADC (Analogue-to-digital converter) unit, which converts the digitized information into voltages that are applied to the X and Y inputs of a cathode ray tube, with a Z-intensify signal applied simultaneously. While the pictures are useful, computer analysis allows for background subtraction, selective contrast enhancement, quantitative output, high resolution, etc. Figures 6 through 9 show pictures and computer outputs of various phantoms. It can be seen that simple schemes of background subtraction yield pictures that are extremely clean.

Work is proceeding in the application of these techniques to clinical uses.

#### Acknowledgments

We would like to thank Miss Ruth Hinkins for her work on the image processing programs. This work was done under the auspices of the U. S. Atomic Energy Commission.

#### References

1. Perez-Mendez, V. and Pfab, J. M., Nucl. Instr. Methods, 33, 141 (1965).
2. Kaufman, L., Perez-Mendez, V., Rindi, A., Sperinde, J. M., and Wollenberg, H. A., "Wire Chambers for Clinical Imaging of Gamma-Rays", Lawrence Radiation Lab Report UCRL-19772, (June 1970). Sub. to Phys. Med. Bio.
3. Rindi, A., Sperinde, J. M., Kaufman L., and Perez-Mendez, V., "Ionization-Triggered Wire Chambers with Magnetostrictive Readout", Lawrence Radiation Lab Report UCID-3271 (October 1968).
4. Kaufman, L., Perez-Mendez, V., and Wollenberg, H., "Applications of Digitized Readout Spark Chambers to Clinical Uses", Lawrence Radiation Lab Report UCID-3184 (June 1968).

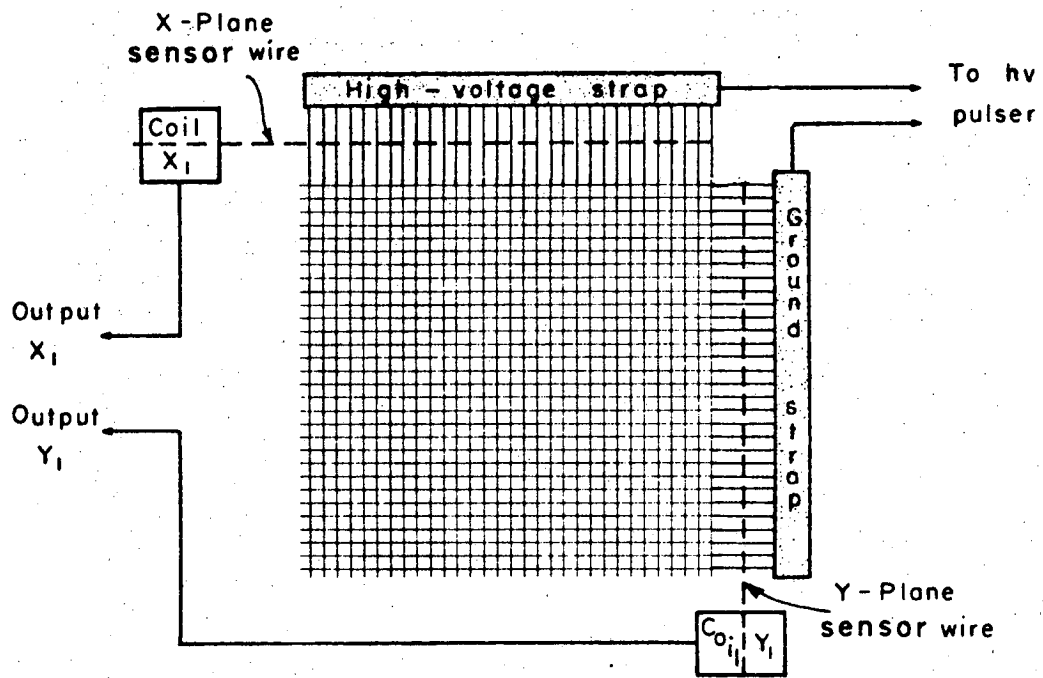


Fig. 1. Schematics of a magnetostrictive readout wire spark chamber.

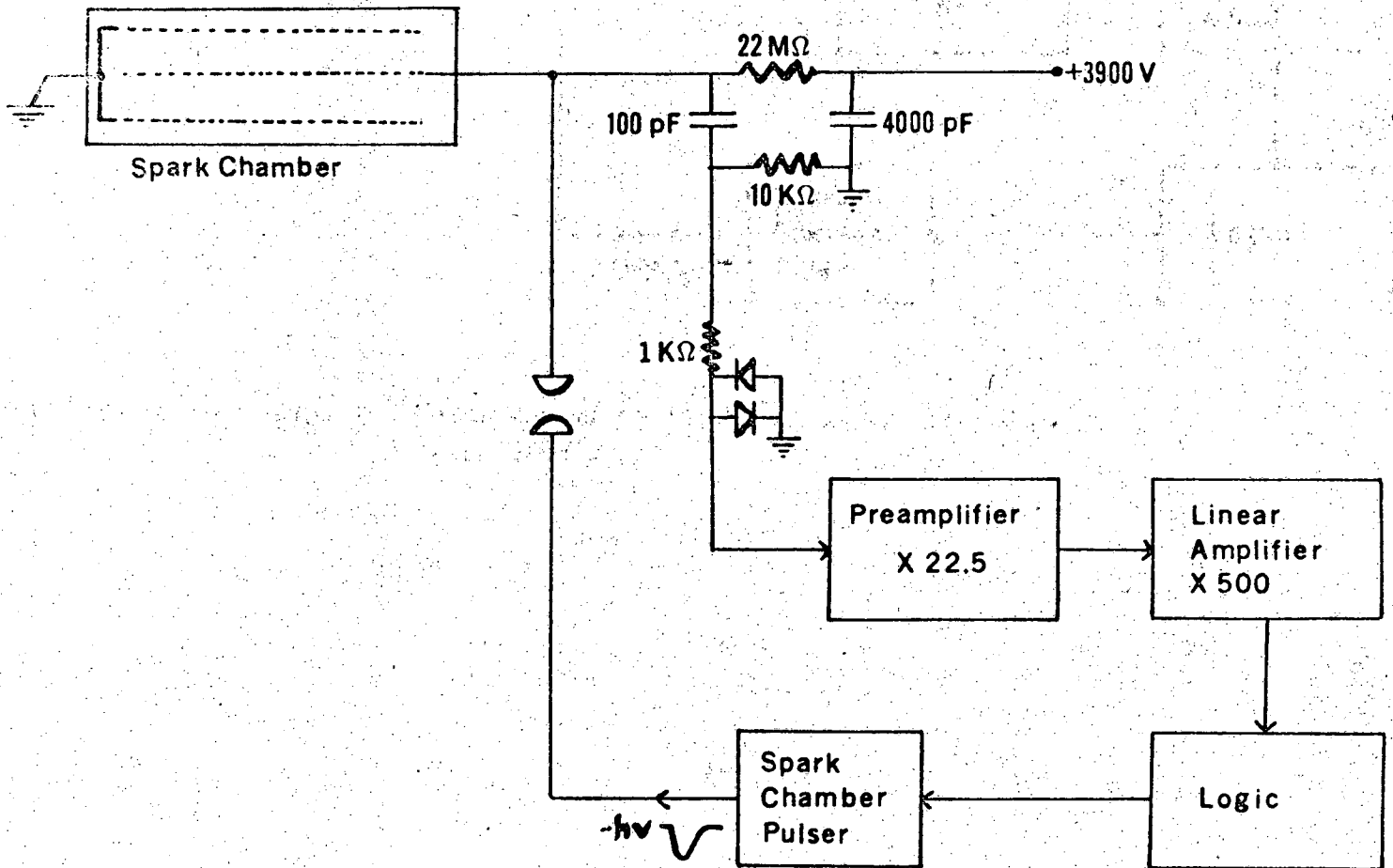
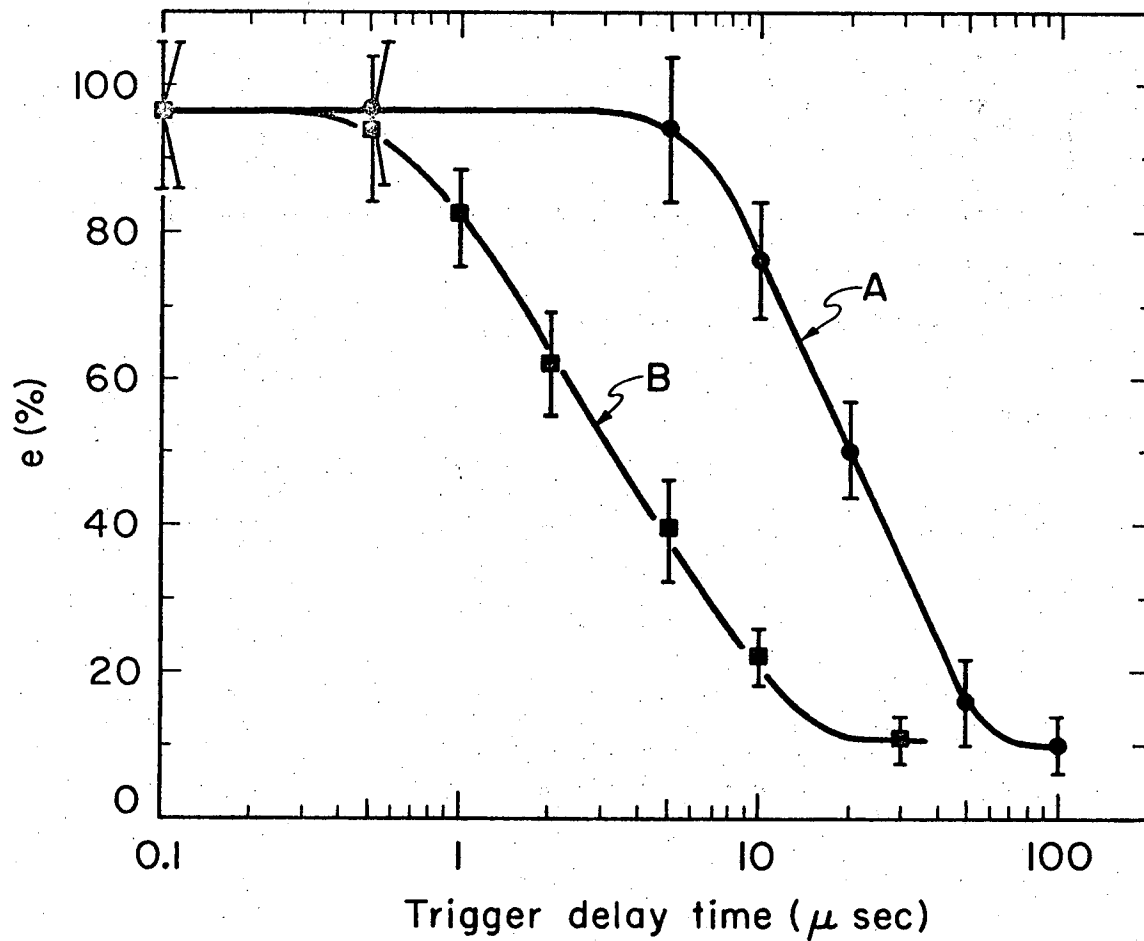


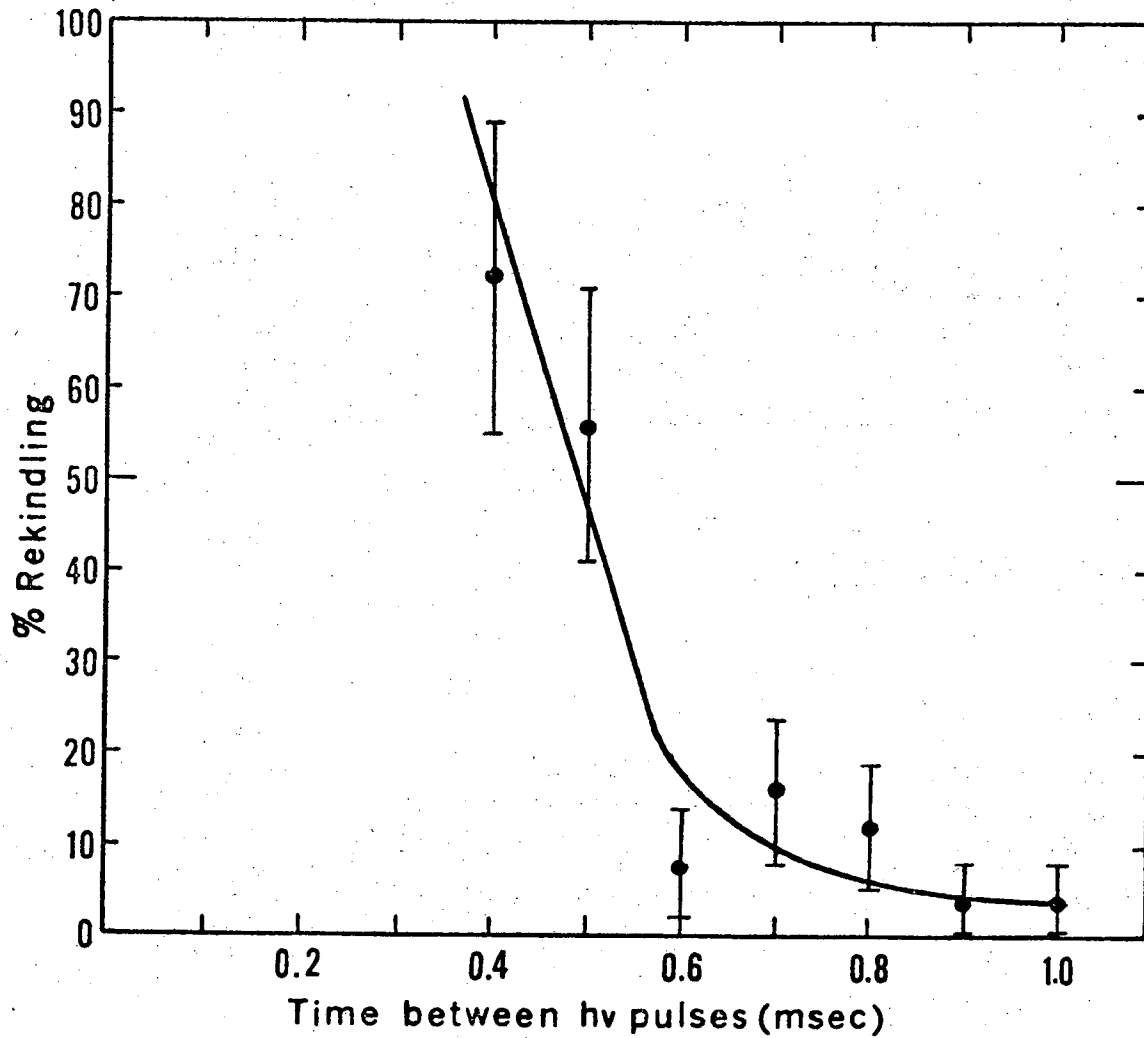
Fig. 2. Setup for gas-multiplication triggering of a spark chamber.



XBL706-3055

Fig. 3. Sparking efficiency as a function of trigger delay. The gas is 90% Ne - 10% He. The delay time is measured after particle detection by the chamber. Curve A is for 3400 V dc and 50 mm Hg of ethanol as the quenching gas; curve B is for 4000 V dc and 215 mm Hg of methanol.





XBL706-3054

Fig. 4. Rekindling of old sparks as a function of time between high-voltage (hv) pulses. Pulsing was done by discharging a 500 pF capacitor at 9 kV. The chamber was flushed at atmospheric pressure with a 90% Ne - 10% He gas mixture saturated with ethyl alcohol ( $\sim 50$  mm Hg).

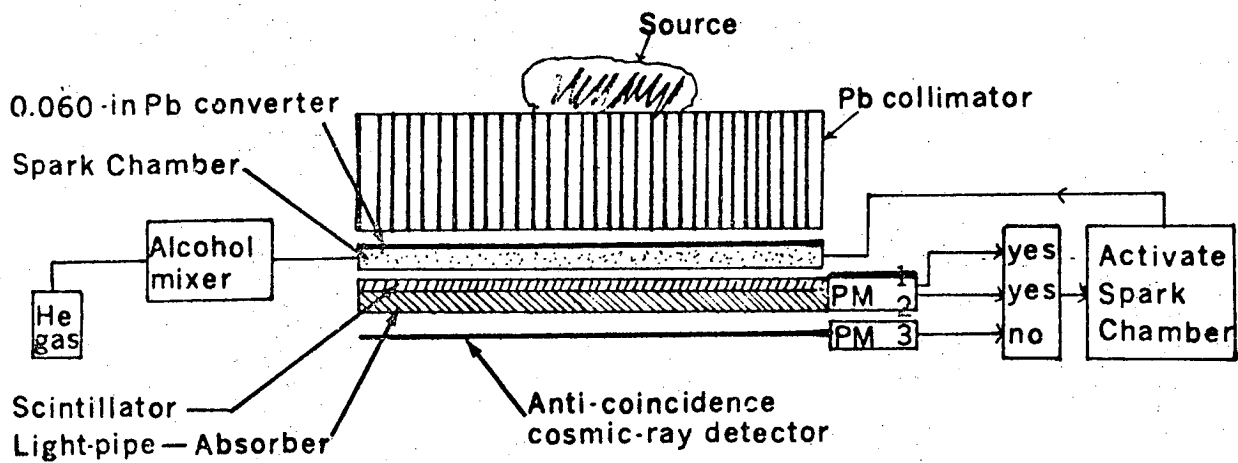
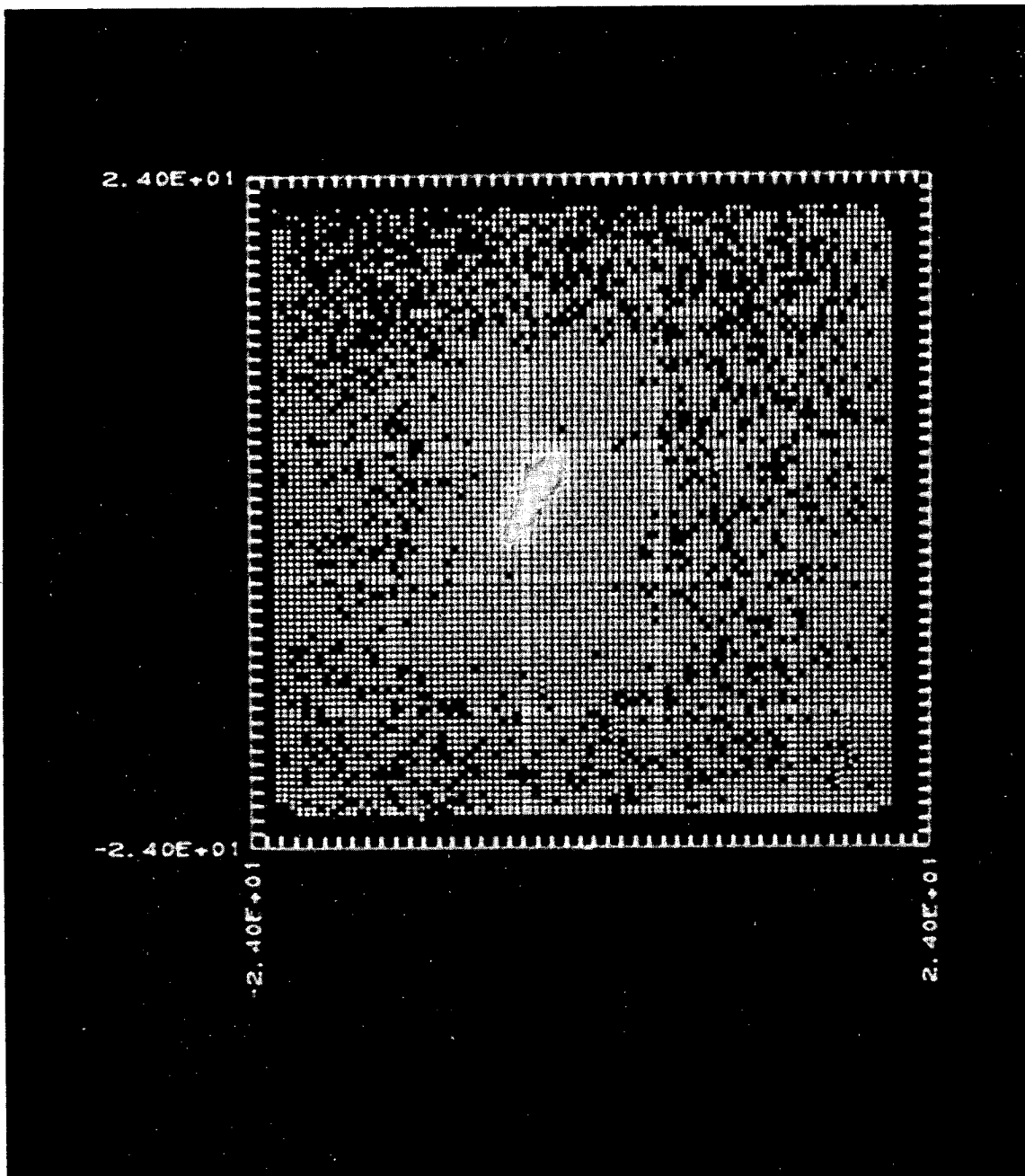
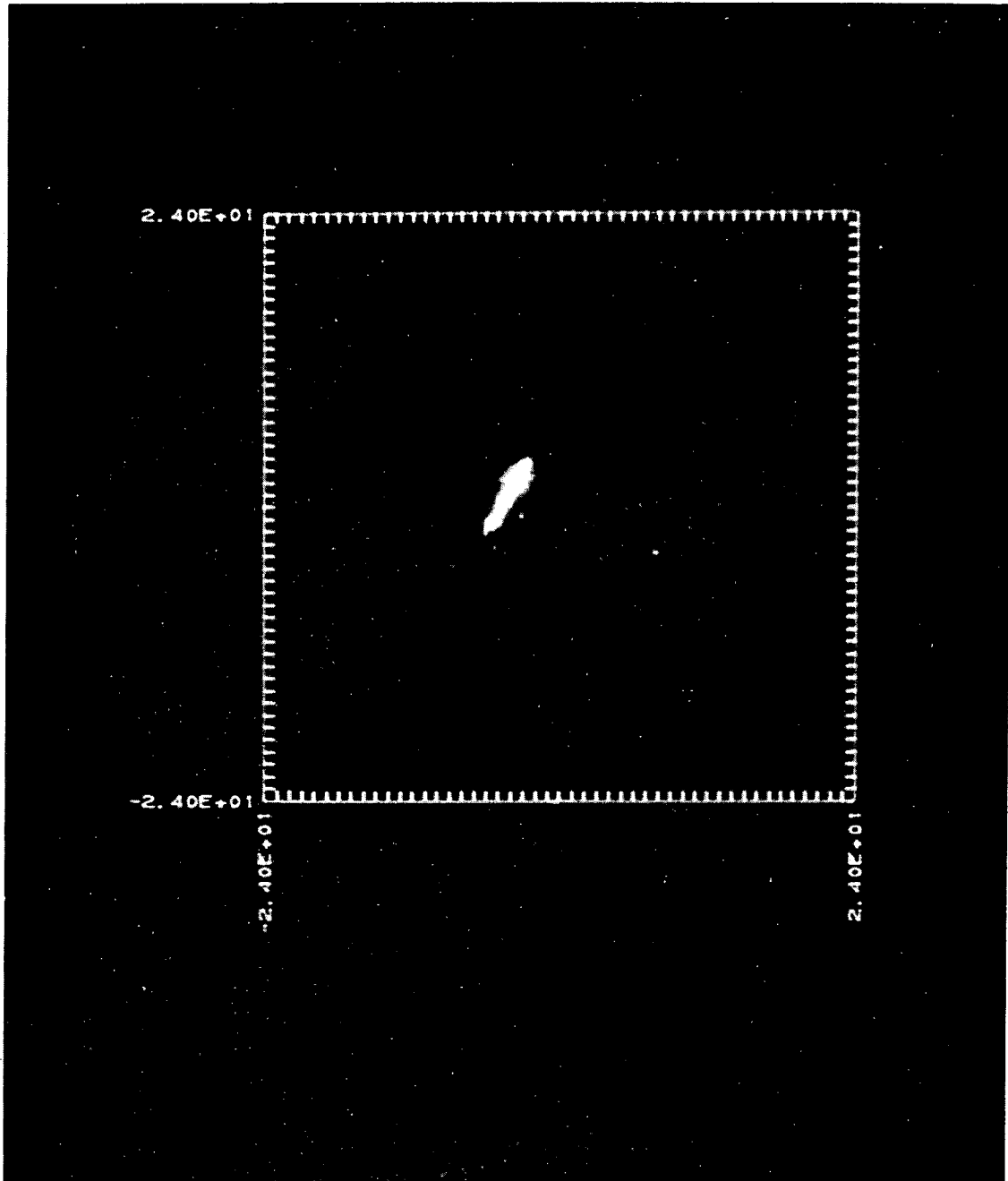


Fig. 5. Schematics of the gamma imaging system in use.



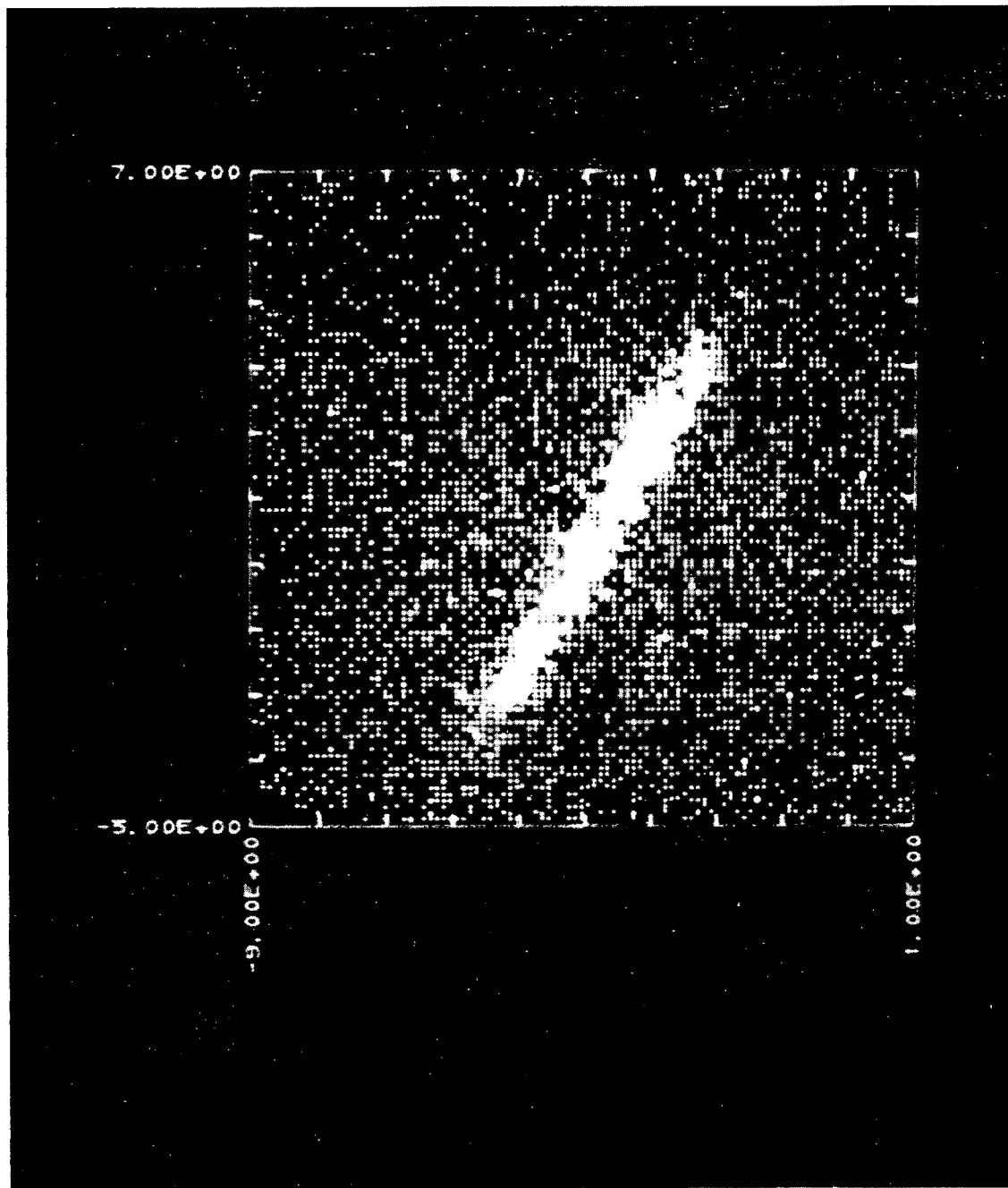
XBB 686-3752

Fig. 6. 0.5 mm - D, 62.5 mm long wire with 50  $\mu\text{Ci}$  of  $\text{Co}^{60}$ . Computer reconstruction of data of the 18" x 18" spark chamber. Lead collimator of 5 mm diameter holes 3 mm septa, and 150 mm thick. 25,000 pts. Scale in centimeters.



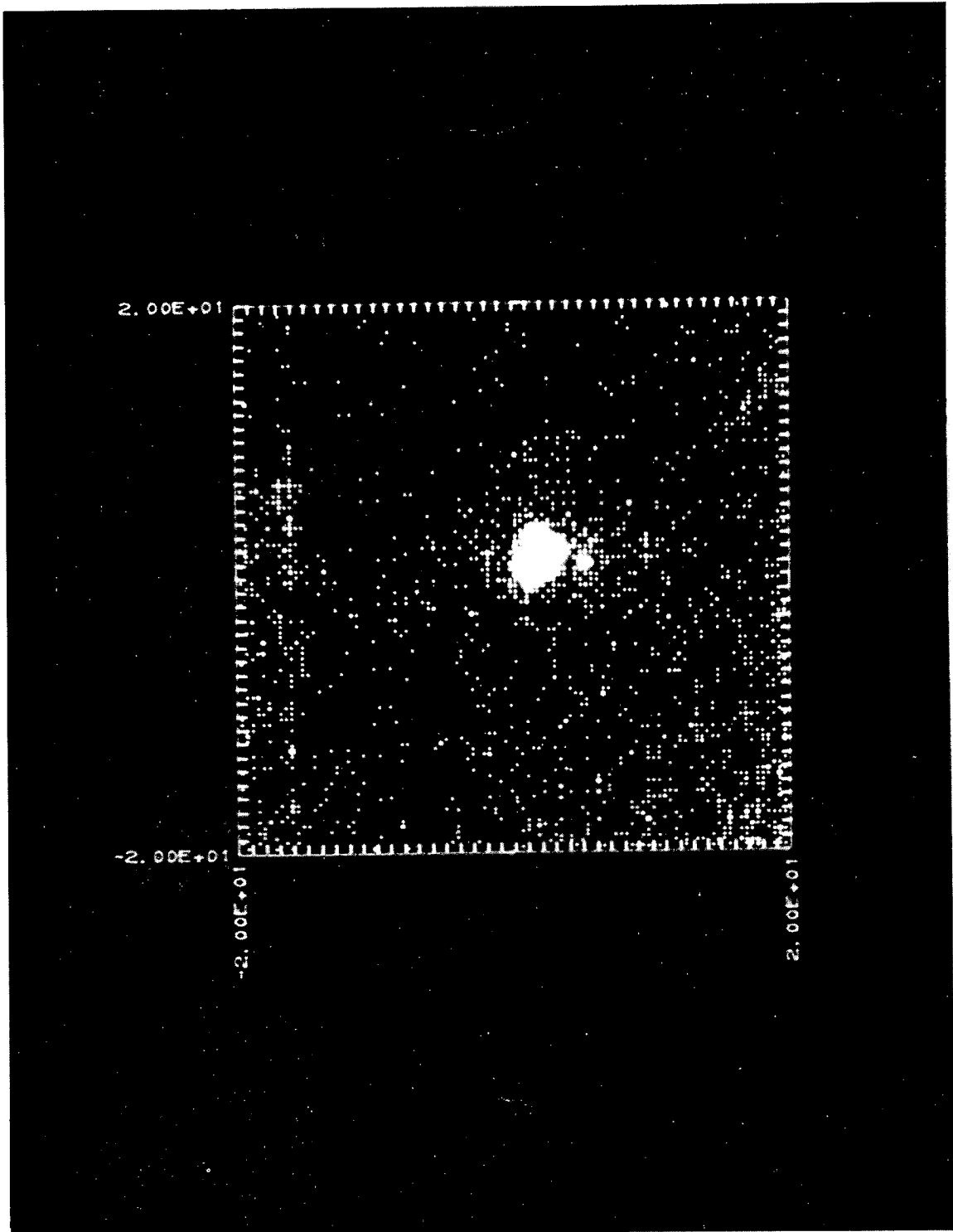
XBB 686-3755

Fig. 7. Same as fig. 6 with 20% background subtraction.



XBB 686-3754

Fig. 8. Expanded view of the area of interest in fig. 6.  
Scale in centimeters.



XBB 686-3753

Fig. 9. Rat's liver and spleen, labeled with  $170 \mu\text{Ci}$  of  $\text{Au}^{198}$ , computer reconstruction of data of the  $18'' \times 18''$  spark chamber, with 20% background subtraction. Lead collimator of 7 mm diameter holes, 5 mm septa and 76 mm thick. 20,000 points. Scale in centimeters.

LEGAL NOTICE

☛ This report was prepared as an account of Government sponsored work. Neither the United States, nor the Commission, nor any person acting on behalf of the Commission:

- A. Makes any warranty or representation, expressed or implied, with respect to the accuracy, completeness, or usefulness of the information contained in this report, or that the use of any information, apparatus, method, or process disclosed in this report may not infringe privately owned rights; or
- B. Assumes any liabilities with respect to the use of, or for damages resulting from the use of any information, apparatus, method, or process disclosed in this report.

As used in the above, "person acting on behalf of the Commission" includes any employee or contractor of the Commission, or employee of such contractor, to the extent that such employee or contractor of the Commission, or employee of such contractor prepares, disseminates, or provides access to, any information pursuant to his employment or contract with the Commission, or his employment with such contractor.

TECHNICAL INFORMATION DIVISION  
LAWRENCE RADIATION LABORATORY  
UNIVERSITY OF CALIFORNIA  
BERKELEY, CALIFORNIA 94720